Wiley Online Library
Early View publication on www.wileyonlinelibrary.com
(issue and page numbers not yet assigned;
citable using Digital Object Identifier – DOI)

J. Biophotonics 1–15 (2016) / **DOI** 10.1002/jbio.201500302

Journal of BIOPHOTONICS

FULL ARTICLE

Improving the quantitative accuracy of cerebral oxygen saturation in monitoring the injured brain using atlas based Near Infrared Spectroscopy models

Michael Clancy[*,1], *Antonio Belli*[2], *David Davies*[2], *Samuel J. E. Lucas*[3], *Zhangjie Su*[2], *and Hamid Dehghani*[4]

[1] PSIBS Doctoral Training Centre, University of Birmingham, United Kingdom
[2] NIHR Surgical Reconstruction and Microbiology Research Centre, Queen Elizabeth Hospital Birmingham, United Kingdom
[3] School of Sport, Exercise and Rehabilitation Science, University of Birmingham, United Kingdom
[4] School of Computer Science, University of Birmingham, United Kingdom

Received 19 November 2015, revised 18 February 2016, accepted 18 February 2016
Published online 23 March 2016

Key words: near infrared spectroscopy, diffuse optical tomography, brain injury

The application of Near Infrared Spectroscopy (NIRS) for the monitoring of the cerebral oxygen saturation within the brain is well established, albeit using temporal data that can only measure relative changes of oxygenation state of the brain from a baseline. The focus of this investigation is to demonstrate that hybridisation of existing near infrared probe designs and reconstruction techniques can pave the way to produce a system and methods that can be used to monitor the absolute oxygen saturation in the injured brain. Using registered Atlas models in simulation, a novel method is outlined by which the quantitative accuracy and practicality of NIRS for specific use in monitoring the injured brain, can be improved, with cerebral saturation being recovered to within $10.1 \pm 1.8\%$ of the expected values.

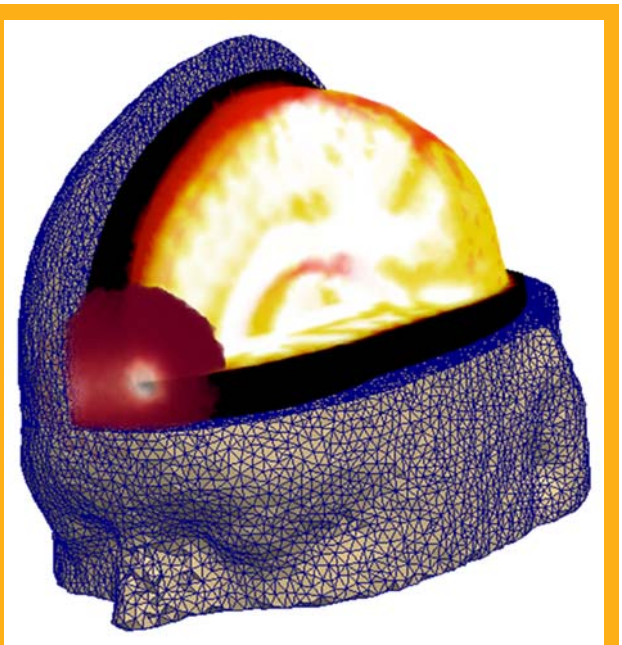

1. Introduction

Traumatic brain injury (TBI) is one of the leading causes of death in young people worldwide [1], with up to 20,000 people sustaining a serious head injury annually [2]. In TBI it is not only the primary brain injury caused by the initial insult which results in the observed high mortality rate (20–40%) [3], but the

* Corresponding author: e-mail: mxc933@bham.ac.uk

variety of hypoxic, ischaemic and cytotoxic events that lead to the profound secondary insult, occurring minutes to hours after the primary event, which poses additional risk to patients [4]. Pathological processes such as the expansion of a mass lesion (i.e., haematoma) may also lead to dangerously high intra cranial pressures which are compounded by the diminished ability of the injured brain to regulate its blood flow to provide adequate perfusion to the cerebral tissues [5]. Therefore an important facet of improving the care of TBI patients is the prediction and prevention of secondary injuries through continuous monitoring in preclinical and clinical locations, so cerebral perfusion can be tightly manipulated externally.

Computer tomography (CT), magnetic resonance imaging (MRI), transcranial Doppler (TCD) and electroencephalography (EEG) are all currently used to monitor brain injury depending on the situation, along with the invasive measurement of intra cranial pressure (ICP) and brain tissue oxygen tension [6]. Consequently, there is no sole technique universally employed to monitor all TBI patients. CT and ICP monitoring are the most commonly used in clinical practice, and although CT is used to identify mass lesions and surgically important pathology, impracticality and ionising radiation make it unsuitable for real-time monitoring and unusable outside the specialist clinical environment. ICP monitors provide long-term, real-time measurements however they are invasive and require surgical implantation. As a non-ionising, non-invasive, cost effective and portable technology, Near Infrared Spectroscopy (NIRS) could provide significant advantages to the monitoring of TBI patients, both in and out of clinical settings [7–9].

Utilising near infrared (NIR) light, consisting of wavelengths ranging from 650–1000 nm [10–12], it is possible to exploit a region of relatively low absorption in biological tissue where scattering becomes the dominant interaction process which allows NIR light to be used to probe several centimetres into tissue and observe biological changes. The non-invasive and non-ionising nature of NIR light has made it a desirable method of imaging and spectroscopy of cerebral and muscular haemodynamics both in research and for clinical applications [13–17]. The fundamental principle when using NIR light is that by measuring the changes of a known input source light, at different wavelengths and detector locations, it is possible to deduce information about the attenuating (scattering and absorption) properties of the medium which then can be used to derive concentrations of chromophores in the target medium. Typically, the main biological chromophores of interest are oxygenated haemoglobin (HbO), deoxygenated haemoglobin (HHb) and water (H_2O), and knowing the relative concentrations of these can provide oxygen saturation measurements and infer information about metabolic activity.

NIRS monitoring of cerebral tissue is widely used during cardiac and vascular surgery, with findings from clinical studies illustrating that a 13–20% drop in saturation is an indicator of post-operative brain tissue damage [18, 19]. In the context of TBI, however, while preliminary work has shown the potential of NIRS, current opinion and clinical practice has not accepted NIRS as a suitable substitute for the invasive measures [15, 20, 21]. Specifically, a correlation between NIRS-derived parameters and other injured brain measures such as CT perfusion and invasive measures of partial oxygen pressure have been reported [22, 23], although as yet this relationship has not been deemed sufficiently robust for NIRS to be used as an independent cerebral tissue monitoring modality. The primary reason for this is that despite the apparent advantages and potential of NIRS in this clinical context, there still remains doubt as to the physical origins of the obtained oxygen saturation values from externally measured optical signals. With the rich vascular nature of facial somatic tissue, questions have been raised about the levels of signal contamination which will occur due to haemodynamic changes in these superficial tissues, obscuring cerebral observations [17, 24–26].

A multitude of different approaches to reduce and/or eliminate superficial contamination have been suggested, ranging from probe design to reconstruction algorithms. The most common design consideration for reducing contamination is to use multi-distant source-detector probe pairs, some very close (~1 cm) to measure only the skin contribution and other probes further apart (2–4 cm) to measure deeper tissue contributions [25]. Given the multi distant data, regression techniques can then be used to filter out the superficial signals. Another common method of reducing contamination is through the use of the spatially resolved spectroscopy (SRS) algorithm [27], which assesses the drop in attenuation over a series of closely spaced detectors in order to produce a tissue oxygenation and tissue haemoglobin index (TOI and THI). Techniques such as SRS do not claim to be quantitatively accurate but instead aim to identify the relative change in oxygen saturation, with the parameter recovery being weighted towards deep tissue signals. In this respect SRS NIRS devices are capable of identifying a relative change in brain saturation during a *Valsalva Manoeuvre* (VM), as demonstrated in previous studies [28, 29], with saturation changes showing the correct magnitude, however the quantitative accuracy of the values never matched the 'expected' values. While these methods have been shown to improve validity of NIRS results it remains apparent that no one technique, so far, has proved sufficient.

As a result of the signal contamination from superficial tissue, the quantitative accuracy of NIRS is therefore limited. The principle of NIRS is that instead of recovering a spatially varying map, it provides a global representation of the optical properties of a target tissue, which makes a quantitative assessment of cerebral oxygenation difficult. Additionally there is a distinct lack of standardisation between different NIRS devices due to the different setups and algorithms used [30], resulting in NIRS experiments to report only changes in baseline measurements. While limiting, this approach is applicable in specific situations such as cardiac surgery and cognitive studies where it can be confidently assumed that the patients' brains are well perfused. In such cases relative changes in cerebral oxygenation can be easily obtained therefore indicators like the aforementioned 13–20% drop in saturation can be reliably observed and used to guide patient care. However in the context of the injured brain, no normative baseline measurements are available as the state of the brain is unknown. Thus a more quantitative measurement of cerebral oxygenation is required in order to gauge the condition of a patient. The main limiting factor is then being the measurement of a global saturation value in the target tissue, which effectively averages the saturation changes over all layers (tissue type) of the head, obscuring the true brain changes.

The progression of NIRS towards a more quantitative assessment of cerebral oxygenation can come in one of two ways. The first is to move to a time domain (TD) NIRS system which maintains the real-time and portable advantages of standard NIRS; however it uses significantly more expensive components capable of individual photon counting. By measuring both intensity and arrival time of the photons, TD NIRS has intrinsic information about photon flight path therefore deep and shallow probing photons can be selected allowing greater quantitative accuracy and increased depth resolution (although still global in the lateral plane) [31].

An alternative method is an adaptation and use of diffuse optical tomography (DOT). DOT differs to conventional NIRS in both system design and reconstruction where instead of the linear probe designs used in NIRS systems consisting of one or two sources and detectors (Figure 1A), a DOT probe will have a larger array (Figure 1B) allowing use of multiple sets of overlapping measurements which can improve both the spatial resolution and quantitative accuracy [32]. Most reconstructions in DOT are model-based, typically using finite element models (FEM) where spatial priors and initial optical property estimates can be used to increase the accuracy of derived optical properties. The limitation of DOT systems is their size and parameter recovery time which makes them less practical for TBI monitoring. Although relative changes in chromophore concentrations from a baseline can be measured in real time, the quantitatively accurate results (of oxygen saturation, for example) require a non-linear and iterative reconstruction approach to hone in on the best solution. To date, however, truly quantitative results have only been obtained in DOT of the breast [33] and the lack of known baseline optical properties in the brain is currently a limiting factor in achieving quantitative results.

Providing spatial priors regarding the tissue layers of the head, namely the skin, bone and brain in a reconstruction algorithm has shown to help constrain the ill-posed nature of the problem and improve parameter recovery accuracy [36]. Such spatial priors can be obtained from patient MRI or CT scans which can be segmented and formed into subject specific models, however in the clinical and pre-clinical setting this is not always a feasible option [32, 36, 37]. Alternatively, the use of atlas-based models has shown good promise to overcome cases where subject specific MRI/CT data are not available [36–38].

Although the application of a DOT-based system can produce the data required to monitor TBI patients, in its current format it is not ideal. The first issue is size and expense of the equipment, which may have a relatively simple solution; the sampled area could be scaled down. Although this would imply a smaller region of interest from which spatially varying parameters would be recovered, such small target regions would be suitable if the results were quantitative. It is worth noting that the invasive ICP

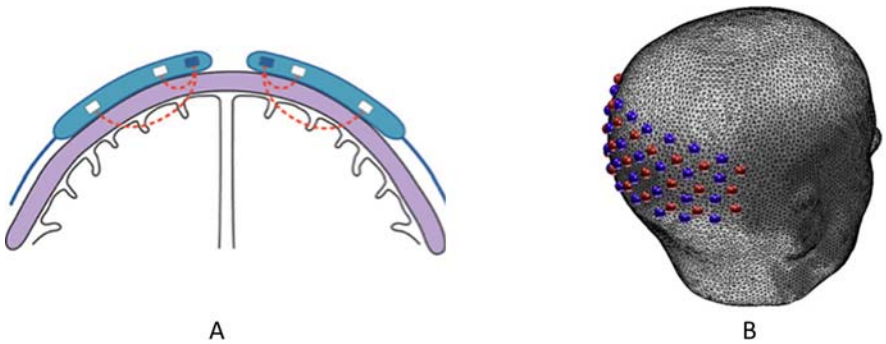

Figure 1 Example of a linear NIRS probe (**A**) and a DOT array (**B**) [34, 35].

probe only target a small area of the brain also. Therefore, if a small DOT probe is used to give overlapping, multi-distant measurements over a small area, it could be used to reconstruct depth resolved spectroscopic parameters. A smaller probe is also more portable and cheaper to produce and will also help with the second issue of reconstruction time. Specifically, smaller the number of voxels (spatially varying locations) being reconstructed, the faster the iterative reconstruction will complete [37]. Also having multiple overlapping measurements obtained over a smaller sample area will improve the ill-posed nature of the inverse problem [39]. With parallel computing and GPU acceleration becoming more prevalent, reconstruction times will only get faster [40], providing additional benefits. The final obstacle in the way of quantitatively accurate DOT reconstructions is the availability of spatial priors. A subject specific reconstruction model will not typically be available in clinical and pre-clinical TBI cases, hence the utilisation of an atlas model, using the average spatial priors over a multitude of segmented heads, could be registered to match a patient head and used as a substitute for specific priors [36, 37].

Finally, while portable high density NIRS system designs are already available and routinely used (e.g., NIRSport, NIRx Medical Technologies and fNIRS300B, BIOPAC System, Inc), the key feature that is currently lacking is the non-trivial base-line parameter recovery needed to obtain information with a reasonable degree of quantitative accuracy. At the other extreme, systems such as the Washington University DOT array [41] uses a large scale probe design, focusing on mapping cerebral activation and connectivity, which incorporate atlas guided recovery into their reconstruction routines. Thus, there are already system designs available that are suitable in terms of hardware. A near infrared system suitable for the monitoring of TBI lies somewhere between these aforementioned designs, hybridising the portability of the smaller DOT arrays with the more enhanced reconstruction algorithms of the large scale probes. While this is something that has been explored [38], there has been limited expansion of the atlas guided techniques to produce quantitatively accurate results. Therefore this study was aimed to investigate the suitability of a small scale DOT probe, designed for use on the forehead, for producing quantitatively accurate cerebral oxygen saturation values, using a registered Atlas model for spatial priors.

2. Methods

In order to assess the quantitative accuracy of DOT reconstruction using registered atlas models, simulations were designed using NIRFAST [10] and a series of simulated brain conditions were constructed to mimic a *Valsalva Manoeuvre* (VM). The VM produces dramatic alterations in ICP, a key parameter monitored in TBI cases (as discussed above). This combined with the fact that the VM will produce very different superficial and cerebral haemodynamic responses makes it an ideal method to test the suitability of NIRS/DOT for TBI monitoring.

2.1 Physiological model

During a VM the subject forces respiratory expiration against a closed glottis, raising intra thoratic pressure. During the initial ~2–3 seconds, perfusion pressure is elevated which is associated with an acute increase in blood flow in the cerebral and systemic circulations [29]. As the VM continues, venous return to the heart is impeded by the raised intra thoratic pressure. This produces a marked reduction in cardiac output and thus blood pressure. The increased intra thoratic pressure also impairs venous outflow from the brain, causing an increase in intra-cranial pressure and venous pooling within the brain and systemic tissue. On release of the VM, the pooled blood is release. Through the dynamic changes in pressure and blood flow, notable changes in both skin and brain haemodynamics are induced (see Figure 2 for simulated predictions based on empirical data [42]). While pressure and flow changes are global, the marked difference in metabolic activity between these cerebral and somatic tissues leads to vastly differing haemodynamic characteristics. As the metabolic demand of cerebral tissue is higher, brain saturation will decrease rapidly as pooling blood is stripped of oxygen to meet demand. The skin, however, will not demonstrate such metabolic activity and its saturation changes closely match the pressure-driven changes in flow across the VM [42]; hence smaller changes in saturation are expected.

2.2 Numerical simulation

The process of data simulation and image reconstruction starts with the creation of subject specific models, the basis of which is a T1 weighted MRI scan (Figure 3A). The MRI scan provides accurate structural information of features within the head, which can be translated into an FEM to accurately predict the propagation of NIR light through the target volume. From this the MRI scans were segmented into 5 separate regions, skin, bone, cerebral spinal fluid (CSF), white matter and grey matter (Figure 3B), using the statistical parametric mapping

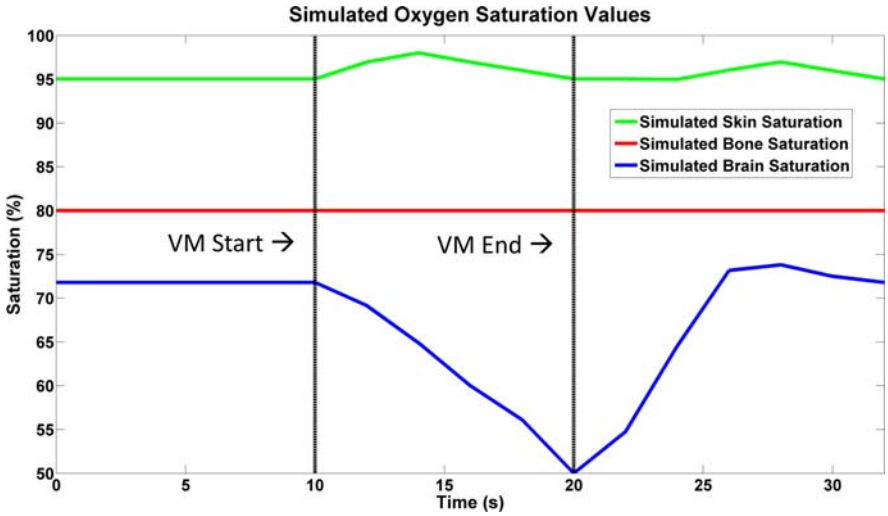

Figure 2 Simulated saturation values for the VM.

(SPM) software package [37, 43] based on a pixel intensity probability function distribution. Following the segmentation of the MRI scans, NIRVIEW [44] was used to create masks of the segmented scans (Figure 3C), on which the final meshing process can be based. NIRVIEW provides a vital checking step to ensure the segmentation process was correct, where any gaps of unassigned pixels can be filled to reduce the risk of holes in the final head model. Small gaps in the segmentation can be rectified using the iterative hole-filling algorithm built into NIRVIEW, which uses a voting algorithm at each iteration to determine where each pixel will be assigned based on the assignment of its surrounding pixels [44]. Large holes that were not filled using the automated routine were filled in manually through inspection of each segmented image slice. The end result of NIRVIEW processing was a stack of segmented masks which could be imported into NIRFAST and used as a basis for volumetric mesh creation (Figure 3D) [10, 44]. Once meshing in NIRFAST was complete, the models could be checked for consistency to ensure there were no holes present in the target forehead region.

Forward (boundary) data for the VM was produced for 9 unique subject models using the FEM-based software package NIRFAST [10], with each time point on Figure 2 providing an individual dataset for a specific set of skin, bone and brain optical properties. The simulation was designed to represent a continuous wave (CW) system so a forward dataset consists of a single boundary intensity measurement for each source-detector pair over three wavelengths.

The DOT probe being modelled (Figure 4) consisted of 8 triple wavelength LED sources (for example, L735/805/850-40C32, Ushio Epitex Inc., Japan) with peaks at 735 nm, 805 nm and 850 nm with a

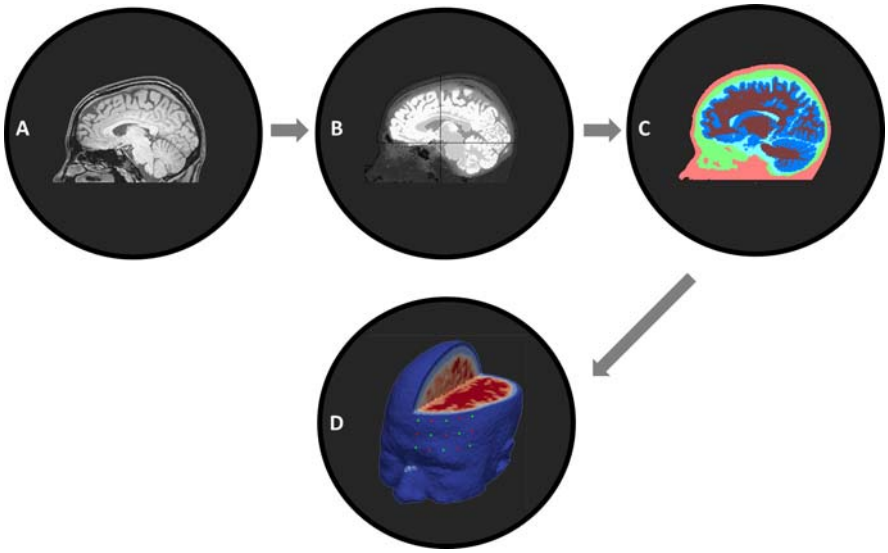

Figure 3 Flow chart of model generation from a patient MRI scan. (**A**) Original T1 weighted MRI scan. (**B**) MRI scan segmented into skin, bone, CSF, white matter and grey matter. (**C**) Masks created in NIRVIEW using the segmented MRI scan. (**D**) Mesh created in NIRFAST using masks.

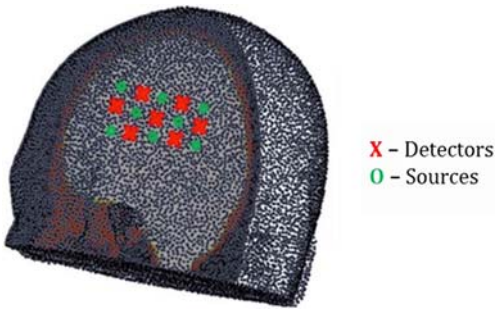

Figure 4 Position and layout of the DOT probe being modelled on the forehead of one example.

bandwidth of 40 nm. There were 7 detectors (for example FDS100, Thorlabs) interspersed within the grid of sources and the spacing between each adjacent source/detector was 15 mm, giving a total of 168 measurements with a minimum source-detector separation of 15 mm and a maximum of 62 mm. In real practical settings the maximum source-detector separation would probably be limited to ~40 mm depending on the dynamic range of the detectors and the systematic noise levels. The probe pad was positioned relative to a user defined reference at the nasion point, as identified from segmented MRI data. From this reference point an iterative positioning algorithm was used to reduce the Euclidean distance between every source and detector to the desired 15 mm over an iterative cycle. From this point inbuilt routines within NIRFAST were used to move the sources one scattering distance beneath the surface of the model to account for the boundary conditions in the diffusion approximation (DA). The baseline optical properties of the atlas head model are shown in Table 1.

A widely used atlas model in DOT studies is the ICBM152 [37, 46, 47], in which studies were primarily designed to look at brain activations and therefore segmentation accuracy was focused on the brain rather than superficial (skin and bone) regions. Our preliminary data showed that there exists a large mismatch between the relative thicknesses of skin and bone within this atlas and subject specific models (see for example Figure 5), with this difference in layer thickness being enough to substantially reduce the accuracy of the model used. Therefore, for the purpose of this work a new atlas was developed based on a tenth subject specific MRI which was segmented (as described above) and used as the new atlas. While the layer thicknesses on the new atlas were more representative of the 9 other models, future work will require a more comprehensive Atlas.

The registration of the Atlas model to each of the 9 subject specific models was achieved using 687 evenly distributed landmarks based on a non-iterative point-to-point (nP2P) algorithm, to minimise the difference between the subject and the Atlas. This method has previously been shown to give a maximum surface registration error of 4.5 mm [37]. While this may appear as a large registration error based on the ~1 mm resolution of the initial MRI scans, it has been shown to be a successful method to provide an alternative to cases where subject specific models are not available [48].

Table 1 Baseline optical properties in Atlas head model [45].

Region	Oxyhaemoglobin (μM)	Deoxyhaemoglobin (μM)	Water (%)	Scatter Power	Scatter Amplitude
Skin	0.0670	0.0035	50	2.82	0.14
Bone	0.0392	0.0098	15	1.47	1.40
Brain	0.0560	0.0220	78	0.76	0.54

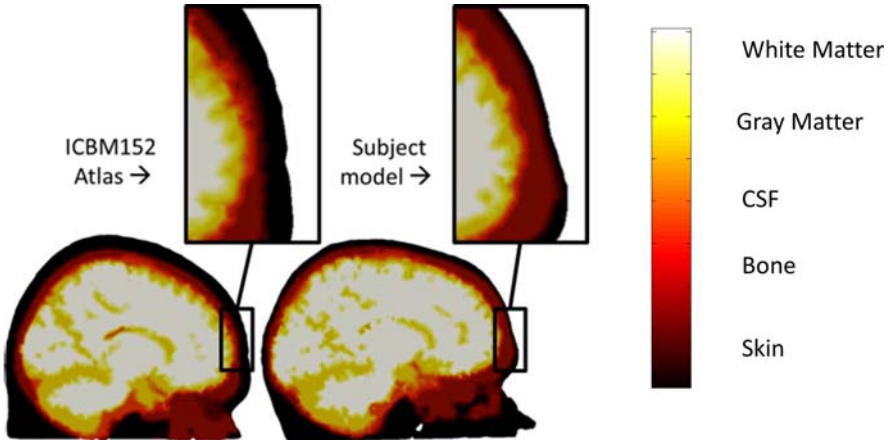

Figure 5 Comparison of the ICBM152 Atlas (Left) and the new Atlas (Right).

The general NIR reconstruction process (the inverse problem) works backwards from a set of boundary data to produce an estimate of the optical properties of the target medium by modelling photon propagation utilising the diffusion approximation as a solution to the radiative transport equation (RTE), which for a CW system is defined by Eq. (1).

$$-D\nabla^2\Phi(\vec{r}) + \mu_a\Phi(\vec{r}) = S(\vec{r}) \quad (1)$$

where $\Phi(\vec{r})$ is the photon fluence at point $\vec{r}$, D is the diffusion coefficient given as $D = 1/3(\mu_a + \mu_s^{'})$. The DA has been shown to be valid in mediums where scatter is the dominant interaction process and the source-detector separations are large enough to allow for multiple scattering events [10]. It may be argued that the use of the DA may not be the most accurate model for application in tomographic imaging of the brain, as there may exist regions where scattering does not dominate absorption (for example Cerebral Spinal Fluid), but the methodologies for parameter recovery outlined here are independent of the model of light propagation utilised.

The DA allows the prediction of NIR light propagation through a medium and the process of recovering optical properties from boundary data can be done in either a single linear step or in a series of nonlinear iterative steps. Linear reconstruction is the simplest and quickest algorithm used for NIRS/DOT systems, typically used to calculate relative changes in chromophore (absorption related) concentrations which has provided a change in measured data from a baseline. The non-linear reconstruction regime is a more complex and time intensive algorithm used for absolute imaging using higher accuracy DOT systems [49]. As the linear reconstruction is a form of difference-based imaging or spectroscopy, which only provides changes relative to a baseline of reference dataset, in this study we focused on using a non-linear, iterative reconstruction process to attempt a quantitatively accurate optical property reconstruction methodology.

Given a head model with coordinates for the position of sources and detectors as well as a set of spatially varying optical properties at each FEM node, the general relationship between the optical properties of a medium and the boundary measurements can be expressed as:

$$\partial y = J\,\partial\mu \quad (2)$$

where ∂y is a change in measurement data (Intensity in this study), J is the Jacobian (or sensitivity matrix) and $\partial\mu$ is the corresponding change in optical properties (absorption related only in this work). With model-based reconstructions using FEM, there is an assigned set of optical properties at every node within the model, therefore Eq. (2) becomes a matrix problem where the matrix J can be inverted and multiplied by the boundary data to obtain an optical property update estimate. The Jacobian is a matrix of values which describes how sensitive the boundary measurements are to a small change in the optical properties at any given node within the model. NIRFAST calculates the Jacobian matrix using the Adjoint method [50], which models light propagation from each source and detector from which a matrix of 'sensitivity' values can be constructed [51]. For a multi-wavelength problem, the structure of the Jacobian matrix is given as:

$$\begin{pmatrix} \partial\Phi_{\lambda 1} \\ \partial\Phi_{\lambda 2} \\ \vdots \\ \partial\Phi_{\lambda n} \end{pmatrix} = \begin{bmatrix} J_{c1,\lambda 1} & J_{c2,\lambda 1} & J_{c3,\lambda 1} & J_{a,\lambda 1} & J_{b,\lambda 1} \\ J_{c1,\lambda 2} & J_{c2,\lambda 2} & J_{c3,\lambda 2} & J_{a,\lambda 2} & J_{b,\lambda 2} \\ & & \vdots & & \\ J_{c1,\lambda n} & J_{c2\lambda n} & J_{c3,\lambda n} & J_{a,\lambda n} & J_{b,\lambda n} \end{bmatrix} \begin{pmatrix} \partial c_1 \\ \partial c_2 \\ \partial c_3 \\ \partial a \\ \partial b \end{pmatrix} \quad (3)$$

where $\partial\Phi$ is the mismatch between measured and simulated data at wavelengths, $\lambda_1 - \lambda_n$ and $c_1 - c_3$ are the Chromophore concentrations with a and b being the scatter amplitude and power, respectively. The scattering power and amplitude are related to the reduced scatter coefficient (μ_s') by an empirical approximation to Mie scattering theory [49] shown in Eq. (4).

$$\mu_s' = a\lambda^{-b} \quad (4)$$

The non-linear reconstruction solves the problem as a series of smaller linear steps (iterations), where at each step a small update in the model optical properties are calculated:

$$J^T(JJ^T + \lambda I)^{-1}\,\partial\Phi = \partial\mu \quad (5)$$

where λ is a regularisation parameter and I is an identity matrix. The iterative process of updating the optical properties continues until a predefined number (40 for all presented data) of iterations or the error between modelled and experimental measurements changes by less than 0.01%.

NIRFAST also allows for a reconstruction basis to be chosen in order to increase computational efficiency. A reconstruction basis allows the model to be subdivided into sections (reconstruction pixels), reducing the number of unknowns in the matrix inversion process (further details found here [52]). Additionally, an increased computational efficiency was obtained by implementing a method of reducing the Jacobian calculation to utilise only sensitivity values greater than 1% of the total sensitivity for parameter recovery [53].

Several different reconstruction regimes were investigated for comparison, including 'inverse crime'

and Atlas-based reconstructions, both utilising 'spatial' priors for either full tomographic or region-based (one value for each layer) parameter recovery. The inverse crime involves using the same FEM for the forward and inverse modelling, which represents an idealised situation in which there is no error in source/detector positioning, the exact scattering properties are known and the spatial information in the model is accurate; whereas the Atlas-based reconstruction provides a more realistic setting. The tomographic reconstructions produce a set of spatially varying optical properties for every node in the FEM, which could then be averaged to give global parameter values per region (skin, bone, brain etc.) post reconstruction. However, the regional reconstructions produce a singular set of optical properties per predefined region, assuming each region is homogeneous. Further details on the region-based reconstruction algorithm can be found elsewhere [54].

The inverse crime reconstructions had the most accurate prior information in terms of spatial and scattering properties; this was designed as a proof-of-concept. Atlas-based reconstructions, however, were designed to assess the ability to reconstruct brain saturation with only an estimate (guess) at absorption, scattering and spatial priors. The chosen reconstruction basis and starting value were kept constant regardless of the reconstruction type for consistency (Table 2).

The reconstruction process itself was split into two steps: (1) a global fit of optical properties based on boundary data for the whole model (i.e. assuming a homogeneous single layer model), which was limited to 20 iterations with a regularisation parameter of 10, and (2) using the bulk average value from the previous step as a basis for either the tomographic or regional reconstruction, which was limited to 40 iteration with a regularisation parameter of 0.01.

For full tomographic-based reconstructions, in order to obtain an average value from each layer, the region of interest for each layer was define as those with a minimum of 2.5% sensitivity, and the reconstructed saturation values were then averaged over these regions of interest. This value was initially chosen based on prior knowledge of photon penetration for the initial homogeneous model, but the importance of model-based, subject-specific modifications are discussed below. For the regional reconstruction a single saturation value was produced for each layer.

3. Results and discussion

3.1 Registration process

The principle of using a registered Atlas model for reconstruction requires that the registration methods applied are capable of giving an accurate fit to the patient-specific models, from which the simulated data are obtained.

The registration accuracy was assessed for each of the 9 models used by measuring the Euclidean distance between nearest neighbour points on the original and registered Atlas models and averaging over all the models (Figure 6). The maximum registration error over the entire head was found to be 22 mm; however this takes into account anomalous regions such as large differences in nose features. Since the main focus of the study was the forehead, the calculated average results confined to the forehead region was found to be less than 10 mm, with errors in the pad region not increasing over 4.53 mm.

With confidence in the accuracy of the registered Atlas models, the next step was to assess the positioning and layout of the DOT probe on the forehead region. The pad-positioning algorithm developed for this work uses a user defined reference point, at the nasion, from which the optode positioning initiates at a fixed x, y and z distance from the nasion. Figure 7 shows the average position of the pads from all models before and after registration, and it can be seen that although the conformity of the pad is correct in the x and z axes, the positioning in the y axis (as controlled by the user defined reference point) is not optimal. This has resulted in a shift of ~5 mm of the pad down the forehead towards the nose, which is not ideal as the probe will be sampling a different region of the cortex. Nevertheless, since the reconstruction averages over the whole pad area, a small change in sample area would be considered negligible in this study, and which represents a more realistic clinical situation where pad orientation and position will vary between patients.

The more important issue however, is the accuracy in layout of the sources and detector positions. If the spacing between sources and detectors used for the reconstruction model is different to that of the original model, there will be inaccuracies which will propagate through to the final reconstructed pa-

Table 2 Optical properties of Atlas and inverse crime models used for reconstruction basis (homogeneous absorption values).

Region	Oxyhaemoglobin (μM)	Deoxyhaemoglobin (μM)	Water (%)	Scatter Power	Scatter Amplitude
Skin	0.0560	0.0140	50	2.82	0.14
Bone	0.0560	0.0140	15	1.47	1.40
Brain	0.0560	0.0140	78	0.76	0.54

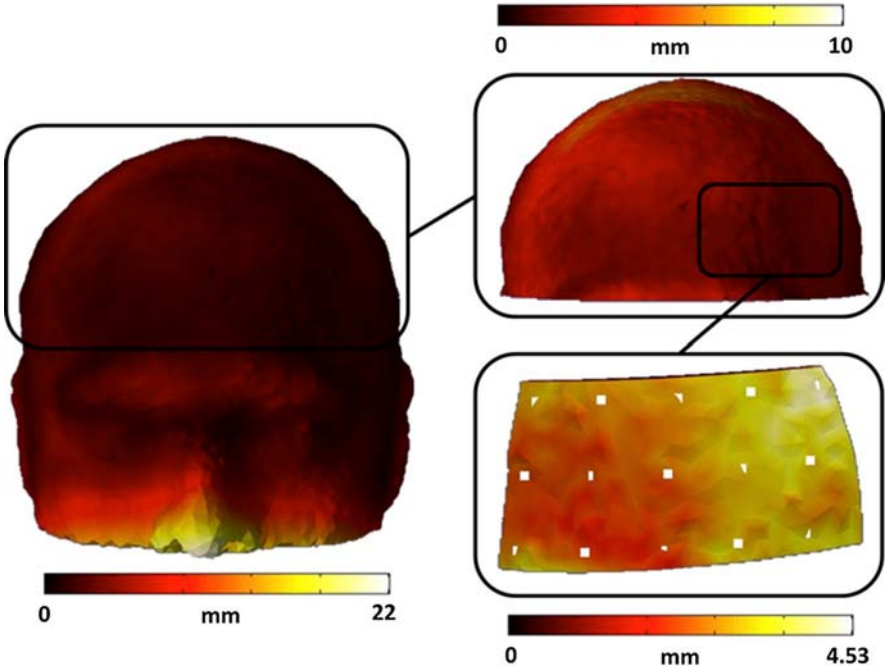

Figure 6 Heat map showing average registration error between each subject specific and the corresponding registered Atlas model (Left). Cropped and rescaled heat map to show registration error on the desired region of interest (forehead) (Top Right). A zoom in on the region of the forehead where DOT pad is positioned (Bottom Right).

rameters. Figure 8 shows a contour plot of positioning accuracy for each source and detector across all the registered models, which was produced by stacking all the pads for all models, aligning their central point and calculating the spread in Euclidian distances between the original location of each source/detector and their position on the registered-Atlas models. This gives a 2D representation of a 3D error. From the plot it can be seen that all the sources and detectors fall within 2.5 mm of their desired position.

Considering the system as a whole, the combination of errors in positioning of the pad and registration of the Atlas models produces a maximum mismatch of 7.5 mm. This is an area where refinements can be made, however, for the scope of the current study this mismatch provides a base level of numerical noise (error) for the reconstruction process, posing a 'worst-case scenario' as a proof-of-concept. In a clinical situation, there will be other confounding factors to reduce the accuracy of the reconstruction, such as detector noise, source variability, poor coupling between the head and probe as well as human error in pad positioning. Human error in pad positioning has be observed in published literature observing the effect of test-retest NIRS studies [55]. Also potential optimisation of the probe positioning through the use of a full head cap is impractical in the context of TBI as there are often bandages and injuries, as well as other invasive probes obstructing the head. These factors are hard to reproduce in simulation; hence the baseline numerical noise from the registration is a good starting point from which future investigations can build and improve upon.

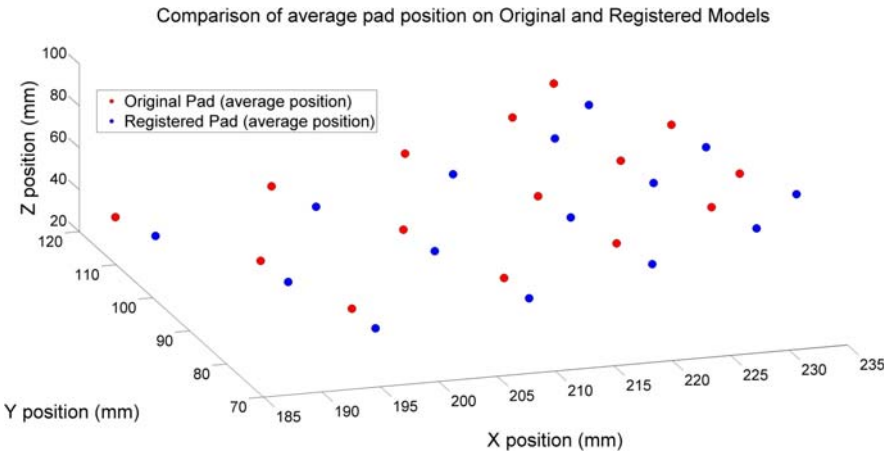

Figure 7 Average coordinates positions of the DOT pad on the original subject-specific models (red) and on the registered-Atlas models (blue).

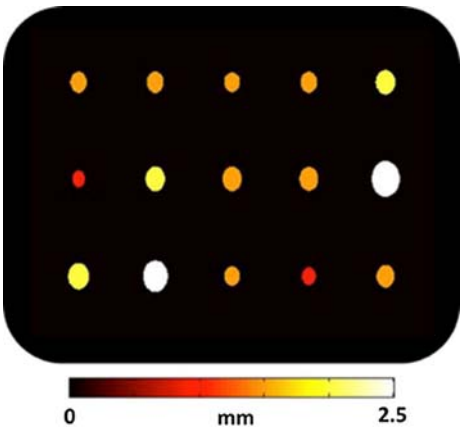

Figure 8 Maximum error in individual source/detector positioning across all the registered-Atlas models. This is a 2D representation of a 3D error.

With regard to the coupling efficiency between the probe and the scalp, as this simulation is designed as a proof of concept, the effect of coupling efficiency has not been considered, however it has been illustrated in other published literature that data can be calibrated to account for intensity and measurement variation effects [56, 57] as well as the recovery of these unknown coefficients as part of the image reconstruction [58], both of which will be subject of further work when considering experimental data.

3.2 *Reconstruction process*

After the registration process, the next step was to assess the reconstruction algorithms and its ability to provide quantitative measures of modelled changes from modelled measurements. The overall quality of the reconstruction was assessed on the accuracy of the recovered saturation values in the brain region, and while ideally all regions would be recovered to the same level of accuracy, in the interest of TBI the main concern is the quantitatively accurate reconstruction of brain saturation. All presented data are the average across all models with error bars showing the standard deviation calculated for across the means of all models.

Reconstructed parameters from all models were analysed in terms of the recovered temporal changes of oxygen saturation for each layer of tissue, as shown in Figure 9. This figure illustrates the recovered values as a function of time shown for the three layers under investigation, namely skin, bone and brain, prior to, during and immediately following a simulated VM. This reconstruction was an 'inverse crime', where the same model was used for both data simulation and reconstruction. From the results shown in Figure 9 it is evident that the region-based reconstruction (where a single parameter is recovered for each tissue type) has given the most accurate results in all three layers of the head. This result demonstrates the validity of the regional reconstruction algorithm (0.04% error for simulated values with a standard deviation of 0.07%), using a set of homogenous starting properties and given accurate spatial priors.

The results when utilising spatially varying tomographic reconstruction are also shown in Figure 9 (blue line), and demonstrate that these do not perform to the same level of accuracy as the region-based reconstructions (green line). Recovered oxygen saturation in the skin, while showing the correct trend, is not quantitatively accurate. Bone region reconstructions show a closer resemblance to the expected changes in the brain rather than for the bone. Finally the brain reconstructions, while showing the correct trends (like the skin), lacked the desired quantitative accuracy, with maximum percentage difference between the average brain parameters and the simulated values of 15.7% (values quoted are percentage error between recovered and simulated values as opposed to a change in oxygen saturation which is also displayed in %) with a standard deviation of 1.2%.

While these tomographic based results are of lower accuracy, they are not unexpected for this set of simulation, since tomography gives a spatially varying saturation value throughout the model in comparison to the region-based reconstructions (Figure 9) which give a single saturation value for an entire region.

To further analyse the tomographic reconstruction, the inaccuracy in the recovered parameters has two main potential factors; firstly the simulation is biased to regional recovery as the simulation itself is for changes that are global to each region. Based on this information it can be speculated that in a clinical situation where changes in each region is heterogeneous, tomography may outperform the regional reconstruction. The second source comes from how each FEM node and its optical properties are selected for averaging. The nodes as discussed earlier are selected in a pre-reconstruction step, where the Jacobian is calculated for the initial homogenous optical properties of the reconstruction model by thresholding to a minimum (at least 2.5%) sensitivity value. A retrospective view would show that this is not the most accurate way to define nodal region of interest. Instead a better method would be to reassesses the Jacobain matrix and the region assignments at the end of each time point reconstruction, and then look at an objective method of thresholding the Jacobian to determine a more accurate region of interest. This way the tomographic reconstruction would be better suited to keep up with any localised changes in sample area due to changes in

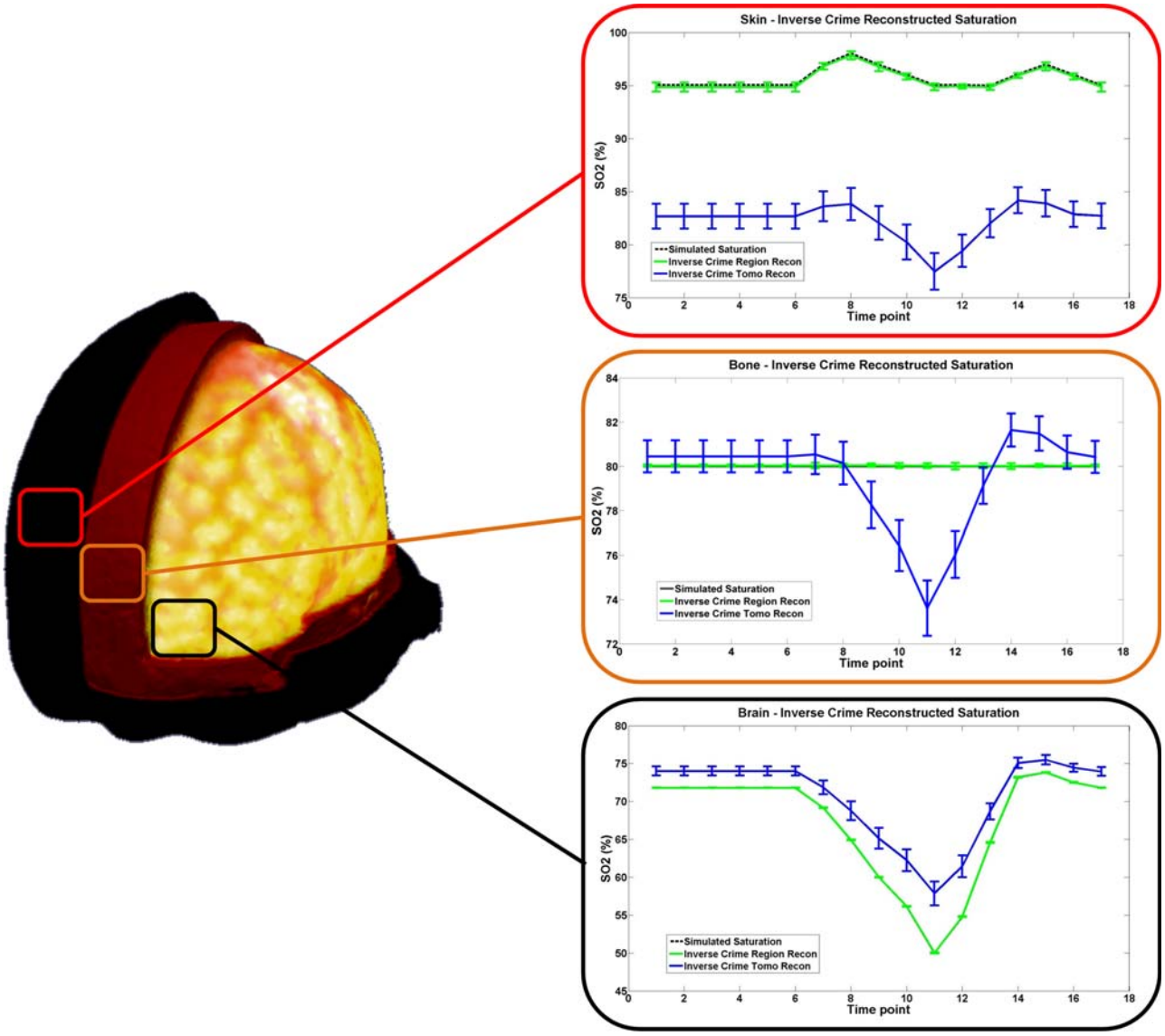

Figure 9 Inverse crime reconstructed saturation values for the skin (top), bone (centre) and brain (bottom) regions (outlined in Figure 2) using both regional (green) and tomography (blue) algorithms prior to, during, and immediately following a VM (time points 6–11) . The plotted results are the average over all models with the error bar showing the standard deviation of the dataset. The simulated saturation line (dashed) in the Brain results graph (bottom graph) is not visible as it overlaps the Inverse Crime Regional Reconstruction (Green) line.

optical properties. For example, Figure 10 shows that as the saturation in the brain decreases the overall sensitivity to the brain region itself is being decreased due to the increased concentration of deoxyhaemoglobin. This is why a decrease in the accuracy of the reconstruction at the peak desaturation of the VM is observed. It would also explain why the bone region is inaccurate around the VM; the change in sensitivity causes cross talk between the brain and bone regions as the region assignment becomes less accurate. In terms of improving the thresholding for region selection, defining a range of values based on a percentage (top 60–95%) of the maximum sensitivity value instead of a simple cut-off sensitivity at 2.5% could offer advantages. As evident in Figure 11, is it clear that by setting only a minimum sensitivity, and not a maximum, the average saturation in the superficial (skin and bone) regions will be inaccurate due to the hot spots of hyper sensitivity.

While the study so far utilising the inverse crime models demonstrate that a small scale DOT probe can be used to obtain quantitatively accurate brain saturation values, it is imperative to investigate the accuracy and validity of using the registered-Atlas models as the basis for the reconstructions, bringing the simulations more in line with clinical conditions

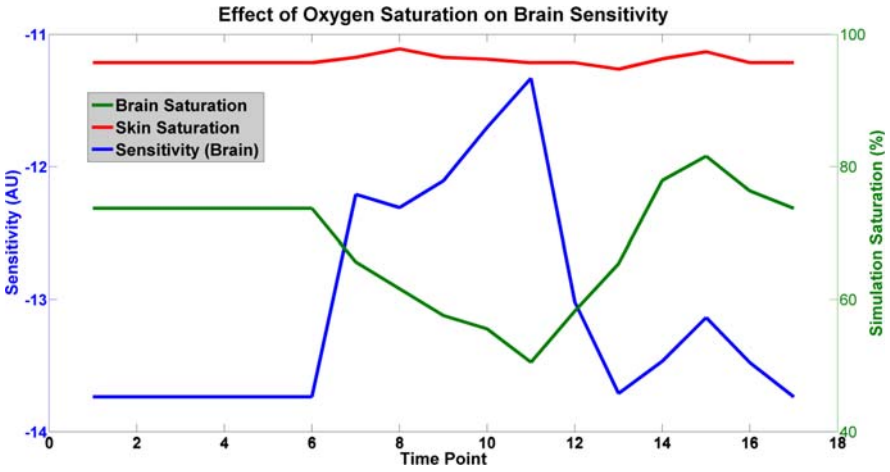

Figure 10 Graph illustrating how the sensitivity of DOT in the brain region alters as the saturation in all regions is varied during the VM. The sensitivity is a summation of the Jacobian values corresponding to brain nodes. More negative values indicate higher sensitivity.

where there is no prior information about the internal structure of the head.

For the regional reconstruction based on registered-Atlas models (Figure 12), the recovered saturation for both skin and bone are subject to poor quantitative accuracy and a large standard deviation. It is evident that fixing spatial priors, by giving absolute spatial information for each region (layer), the reconstruction is not able to accurately recover the superficial saturation values. This indicates that despite the utilisation of the new Atlas model, the variation in superficial layer thickness between subjects and the Atlas is still confounding the reconstructions. Evidence of this cross talk within the superficial layers can also be seen with a simple comparison of the trends in the skin and bone regions, which both appear to follow the same trends as the simulated skin saturations, thus implying that the skin layer is too thin in the utilised Atlas model. Despite the mismatch in superficial layers, the region-based reconstruction recovered the brain saturation values with an average percentage difference of 11.2% (standard deviation – 5.0%) between simulated and reconstructed values. While this does not seem overly accurate, in comparison to some of the existing NIRS techniques such as SRS reconstructions explored in previous work [16, 28, 59, 60], region-based DOT shows a marked improvement.

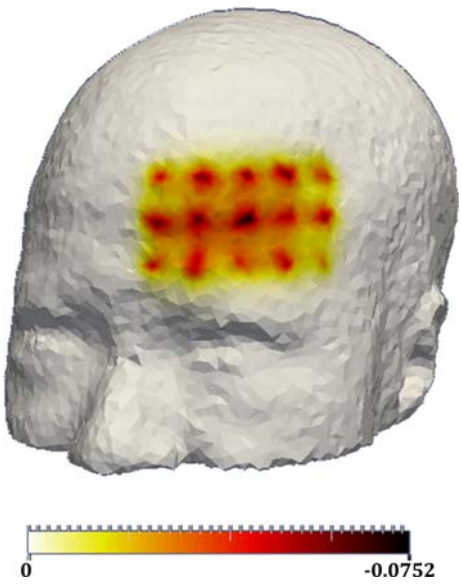

Figure 11 Plot of Jacobian (sensitivity) matrix values on the surface of a subject-specific model showing the 'hot spots' of hyper sensitivity under each of the sources and detectors. A smaller sensitivity value represents a higher sensitivity.

Unlike the inverse crime reconstructions, once the Atlas is employed, the quality of the tomographic reconstruction surpassed that of the regional in all layers, other than the skin (see Figures 9 and 12) in terms of both quantitative accuracy and the standard deviation of the recovered saturation values. The average percentage difference between the simulation and reconstructed brain values was 10.1% with a standard deviation of 1.8%. While the fixed region sizes posed an issue for the regional reconstructions, the tomographic process was not constricted in the same way. The Atlas tomography even performed better than its inverse crime counterpart, again highlighting issues with region of interest (ROI) selection. The limiting factors in grouping nodes into a ROI via Jacobian thresholding still apply, however because of the mismatch in superficial layer size these errors appear to average out over the course of all the head models, smoothing the results.

The main consideration when assessing the quality of the registered-Atlas reconstructions is that the results were more quantitatively accurate than the current NIRS-based recovery techniques. While absolute quantification was never anticipated, the main goal of this study was to show the potential of DOT to improve on current NIRS limitations, which is clearly visible from the above results.

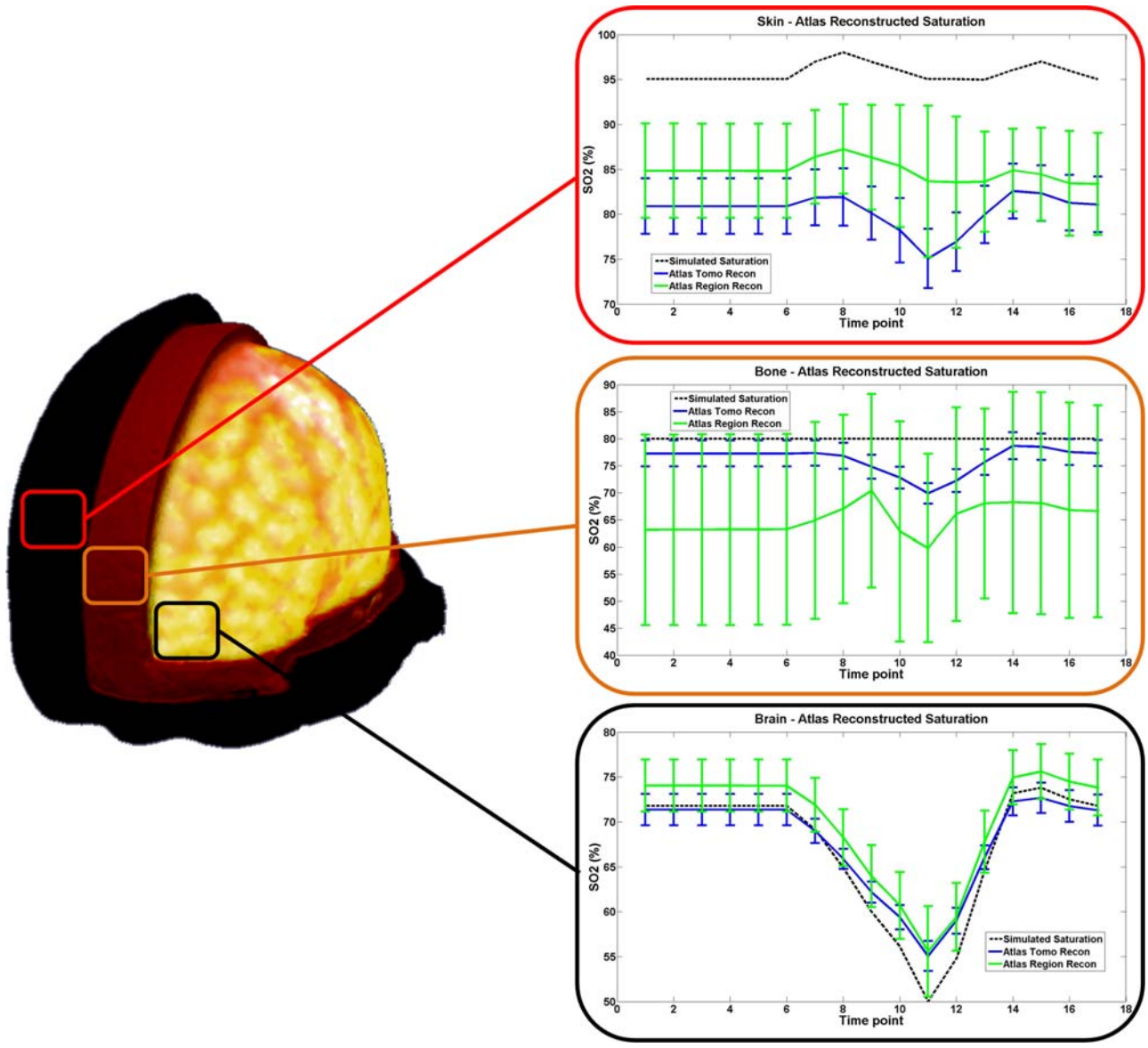

Figure 12 Atlas reconstructed saturation values for the skin (top), bone (centre) and brain (bottom) regions using both regional (green) and tomography (blue) algorithms. The plotted results are the average over all models with the error bar showing the standard deviation of the dataset.

4. Conclusion

Currently the NIRS technology that is available in the clinic lacks the quantitative accuracy to monitor saturation changes in TBI patients. The global measures of saturation provided by NIRS probes mean that the target changes in the brain are often confounded by the haemodynamics of superficial layers such as skin and bone. While brain haemodynamic changes are observable, the saturation values obtained are not reliable enough to allow NIRS to be used as a clinical gold standard for TBI monitoring.

In the context of measuring quantitatively accurate brain saturation measurements in TBI patients, the technique of Atlas-guided reconstructions has shown significant potential. While there are many refinements to both the reconstruction algorithms and the realism of the simulations, which can be made, the data in this study present a 'first step' towards clinical DOT measurements for TBI monitoring. Where previous studies implementing NIRS into the clinic have found that the superficial saturation changes can obscure accurate brain observation, current simulations for DOT have shown the potential

benefits. Due to the iterative recovery process of DOT it is inherent that more prior information can be provided. Even though this information has proved inaccurate in terms of superficial layer size, the known depth of the cortex surface (roughly constant over all heads) has allowed for significant improvements in brain parameter recovery.

The next progression of this work comes in two forms. The first needs to focus on the refinement of the reconstruction techniques. This will come in the form of redeveloping the Atlas so that the superficial layer mismatch provides less of an issue. Also in terms of improving the tomography reconstructions, thorough investigations into methods of selecting the correct regions of interest are required. The second is the practical implementation for a clinical DOT NIRS system. Simulations will never truly mimic clinical conditions, thus the probe needs to be characterised and tested on a mix of, well defined phantom models, healthy volunteers and TBI patients.

Acknowledgements This work was supported by EPSRC grant EP/50053X/1 and the United Kingdom National Institute for Health Research – Surgical Reconstruction and Microbiology Centre (NIHR SRMRC).

This paper was amended 6 April 2016 after initial publication. Figure 9 was altered.

References

[1] M. F. Stiefel, A. Spiotta, V. H. Gracias, A. M. Garuffe, O. Guillamondegui, E. Maloney-Wilensky, S. Bloom, M. S. Grady, and P. D. LeRoux, Journal of Neurosurgery **103**(5), 805–811 (2005).
[2] S. Hodgkinson, V. Pollit, C. Sharpin, and F. Lecky, Bmj **348** (2014).
[3] E. Maloney-Wilensky, V. Gracias, A. Itkin, K. Hoffman, S. Bloom, W. Yang, S. Christian, and P. D. LeRoux, Critical Care Medicine **37**(6), 2057–2063 (2009).
[4] D. F. Signorini, P. J. Andrews, P. A. Jones, J. M. Wardlaw, and J. D. Miller, Journal of Neurology, Neurosurgery & Psychiatry **66**(1), 26–31 (1999).
[5] J. J. Fletcher, K. Bergman, P. A. Blostein, and A. H. Kramer, Neurocritical Care **13**(1), 47-56 (2010).
[6] J. Ghajar, The Lancet **356**(9233), 923–929 (2000).
[7] T. Muehlemann, D. Haensse, and M. Wolf, Optics Express **16**(14), 10323–10330 (2008).
[8] E. Lareau, F. Lesage, P. Pouliot, D. Nguyen, J. Le Lan, and M. Sawan, Journal of Biomedical Optics **16** (9), 096014 (2011).
[9] S. Perrey, Methods **45**(4), 289–299 (2008).
[10] H. Dehghani, M. E. Eames, P. K. Yalavarthy, S. C. Davis, S. Srinivasan, C. M. Carpenter, B. W. Pogue, and K. D. Paulsen, Communications in Numerical Methods in Engineering **25**(6), 711–732 (2009).
[11] T. Durduran, R. Choe, W. Baker, and A. Yodh, Reports on Progress in Physics **73**(7), 076701 (2010).
[12] M. Ferrari and V. Quaresima, Neuroimage **63**(2), 921–935 (2012).
[13] A. F. Abdelnour and T. Huppert, Neuroimage **46**(1), 133–143 (2009).
[14] Y. Hambhani, Journal of Near Infrared Spectroscopy **20**, 117–139 (2012).
[15] S. R. Leal-Noval, A. Cayuela, V. Arellano-Orden, A. Marín-Caballos, V. Padilla, C. Ferrándiz-Millón, Y. Corcia, C. García-Alfaro, R. Amaya-Villar, and F. Murillo-Cabezas, Intensive Care Medicine **36**(8), 1309–1317 (2010).
[16] M. Clancy, A. Belli, D. Davies, S. J. E. Lucas, Z. Su, and H. Dehghani, Comparison of neurological NIRS signals during standing Valsalva maneuvers, pre and post vasoconstrictor injection. In: European Conferences on Biomedical Optics. 2015. International Society for Optics and Photonics.
[17] D. J. Davies, Z. Su, M. Clancy, S. Lucas, H. Dehghani, A. Logan, and A. Belli, http://www.wieland.sportwelt.at/ Journal of Neurotrauma, 2015(ja), 2015.
[18] P. G. Al-Rawi and P. J. Kirkpatrick, Stroke **37**(11), 2720–2725 (2006).
[19] T. Scheeren, P. Schober, and L. Schwarte, Journal of Clinical Monitoring and Computing **26**(4), 279–287 (2012).
[20] A. Ghosh, C. Elwell, and M. Smith, Anesthesia & Analgesia **115**(6), 1373–1383 (2012).
[21] Y. Hoshi, Psychophysiology **40**(4), 511–520 (2003).
[22] P. Taussky, B. O'Neal, W. P. Daugherty, S. Luke, D. Thorpe, R. A. Pooley, C. Evans, R. A. Hanel, and W. D. Freeman, Neurosurgical Focus **32**(2), E2, (2012).
[23] K. Budohoski, C. Zweifel, M. Kasprowicz, E. Sorrentino, J. Diedler, K. Brady, P. Smielewski, D. Menon, J. Pickard, and P. Kirkpatrick, British Journal of Anaesthesia **108**(1), 89–99 (2012).
[24] S. L. Ferradal, B. R. White, R. Dosenbach, and J. P. Culver. Bedside Monitoring of Cerebral Oxygenation Using DOT. in Digital Holography and Three-Dimensional Imaging. Optical Society of America (2010).
[25] L. Gagnon, M. A. Yücel, D. A. Boas, and R. J. Cooper, Neuroimage **85**, 127–135 (2014).
[26] M. Ferrari, L. Mottola, and V. Quaresima, Canadian Journal of Applied Physiology **29**(4), 463–487 (2004).
[27] S. Suzuki, S. Takasaki, T. Ozaki, and Y. Kobayashi. Tissue oxygenation monitor using NIR spatially resolved spectroscopy. in BiOS'99 International Biomedical Optics Symposium. International Society for Optics and Photonics (1999).
[28] M. Clancy, A. Belli, D. Davies, S. J. E. Lucas, Z. Su, and H. Dehghani. Monitoring the Injured Brain – Registered, patient specific Atlas models to improve accuracy of recovered brain saturation values. in European Conference of Biomedical Optics. Munich (2015).
[29] B. G. Perry, T. Mündel, D. J. Cochrane, J. D. Cotter, and S. J. Lucas, Physiological Reports **2**(2), e00233 (2014).
[30] M. Ferrari and V. Quaresima, J. Near Infrared Spectrosc **20**(1), 1–14 (2012).

[31] A. Torricelli, D. Contini, A. Pifferi, M. Caffini, R. Re, L. Zucchelli, and L. Spinelli, Neuroimage **85**, 28–50 (2014).
[32] D. A. Boas, A. M. Dale, and M. A. Franceschini, Neuroimage **23**, S275–S288 (2004).
[33] B. W. Pogue, S. P. Poplack, T. O. McBride, W. A. Wells, K. S. Osterman, U. L. Osterberg, and K. D. Paulsen, Radiology **218**(1), 261–266 (2001).
[34] A. T. Eggebrecht, B. R. White, S. L. Ferradal, C. Chen, Y. Zhan, A. Z. Snyder, H. Dehghani, and J. P. Culver, Neuroimage **61**(4), 1120–1128 (2012).
[35] S. N. Davie and H. P. Grocott, Anesthesiology **116**(4), 1–1 (2012).
[36] R. J. Cooper, M. Caffini, J. Dubb, Q. Fang, A. Custo, D. Tsuzuki, B. Fischl, W. Wells, I. Dan, and D. A. Boas, Neuroimage **62**(3), 1999–2006 (2012).
[37] X. Wu, A. T. Eggebrecht, S. L. Ferradal, J. P. Culver, and H. Dehghani, Biomedical Optics Express **5**(11), 3882–3900 (2014).
[38] A. Custo, D. A. Boas, D. Tsuzuki, I. Dan, R. Mesquita, B. Fischl, W. E. L. Grimson, and W. Wells, Neuroimage **49**(1), 561–567 (2010).
[39] D. Boas, D. H. Brooks, E. L. Miller, C. DiMarzio, M. Kilmer, R. J. Gaudette, and Q. Zhang, Signal Processing Magazine, IEEE **18**(6), 57–75 (2001).
[40] M. Schweiger, Journal of Biomedical Imaging **2011**, 10 (2011).
[41] A. T. Eggebrecht, S. L. Ferradal, A. Robichaux-Viehoever, M. S. Hassanpour, H. Dehghani, A. Z. Snyder, T. Hershey, and J. P. Culver, Nature Photonics **8**(6), 448–454 (2014).
[42] D. J. Davies, Z. Su, M. Clancy, S. Lucas, H. Dehghani, A. Logan, A. Belli, and S. Lucas, Reliable cerebral haemodynamic signals detected by near infra-red spectroscopy; reduction in skin blood flow has minimal effect, 2015.
[43] K. J. Friston, Statistical parametric mapping, in Neuroscience Databases, Springer, pp. 237–250 (2003).
[44] M. Jermyn, H. Ghadyani, M. A. Mastanduno, W. Turner, S. C. Davis, H. Dehghani, and B. W. Pogue, Journal of Biomedical Optics **18**(8), 086007 (2013).
[45] H. Dehghani, B. R. White, B. W. Zeff, A. Tizzard, and J. P. Culver, Applied Optics **48**(10), D137–D143 (2009).
[46] J. Mazziotta, A. Toga, A. Evans, P. Fox, J. Lancaster, K. Zilles, R. Woods, T. Paus, G. Simpson, and B. Pike, Journal of the American Medical Informatics Association **8**(5), 401–430 (2001).
[47] J. Mazziotta, A. Toga, A. Evans, P. Fox, J. Lancaster, K. Zilles, R. Woods, T. Paus, G. Simpson, and B. Pike, Philosophical Transactions of the Royal Society B: Biological Sciences **356**(1412), 1293–1322 (2001).
[48] S. L. Ferradal, A. T. Eggebrecht, M. Hassanpour, A. Z. Snyder, and J. P. Culver, Neuroimage **85**, 117–126 (2014).
[49] H. Dehghani, S. Srinivasan, B. W. Pogue, and A. Gibson, Philosophical Transactions of the Royal Society of London A: Mathematical, Physical and Engineering Sciences **367**(1900), 3073–3093 (2009).
[50] S. R. Arridge and M. Schweiger, Applied Optics **34** (34), 8026–8037 (1995).
[51] L. V. Wang and H.-I. Wu, Biomedical optics: principles and imaging, John Wiley & Sons (2012).
[52] S. C. Davis, H. Dehghani, J. Wang, S. Jiang, B. W. Pogue, and K. D. Paulsen, Optics Express **15**(7), 4066–4082 (2007).
[53] M. E. Eames, B. W. Pogue, P. K. Yalavarthy, and H. Dehghani, Optics Express **15**(24), 15908–15919 (2007).
[54] H. Dehghani, B. W. Pogue, J. Shudong, B. Brooksby, and K. D. Paulsen, Applied Optics **42**(16), 3117–3128 (2003).
[55] A. Blasi, S. Lloyd-Fox, M. H. Johnson, and C. Elwell, Neurophotonics **1**(2), 025005 (2014).
[56] K. E. Michaelsen, V. Krishnaswamy, L. Shi, S. Vedantham, S. P. Poplack, A. Karellas, B. W. Pogue, and K. D. Paulsen, Biomedical Optics Express **6**(12), 4981–4991 (2015).
[57] H. Dehghani, B. W. Pogue, S. P. Poplack, and K. D. Paulsen, Applied Optics **42**(1), 135–145 (2003).
[58] D. Boas, T. Gaudette, and S. Arridge, Optics express **8**(5), 263–270 (2001).
[59] M. Clancy, A. Belli, D. Davies, S. J. E. Lucas, Z. Su, and H. Dehghani. Evaluating Depth Dependency in Functional Near Infrared Spectroscopy (fNIRS) for Human Brain Study. OSA Biomedical Optics Conference (2014).
[60] M. Clancy, A. Belli, D. Davies, S. J. E. Lucas, Z. Su, and H. Dehghani. Evaluation of Spatially Resolved Spectroscopy (SRS) in Traumatic Brain Injury (TBI). in fNIRS2014. Montreal (2014).